Arabian Journal of Chemistry (2016) 9, S548–S556

King Saud University

Arabian Journal of Chemistry

www.ksu.edu.sa
www.sciencedirect.com

ORIGINAL ARTICLE

Pharmacological and spectral studies of synthetic biomimetic copper complexes derived from 3-hydroxyflavone derivatives as anti-inflammatory agents

K. Nagashri [a], J. Joseph [a,*], C. Justin Dhanaraj [b]

[a] Department of Chemistry, Noorul Islam Centre for Higher Education (Noorul Islam University), Kumaracoil 629 180, India
[b] Department of Chemistry, Anna University Tirunelveli, University VOC College of Engineering, Thoothukudi, India

Received 22 March 2011; accepted 21 June 2011
Available online 29 June 2011

KEYWORDS

Antimicrobial;
Serial dilution;
Anti-inflammatory;
Lead;
Superoxide

Abstract Novel biomimetic ligands were synthesized by the condensation of 3-hydroxyflavone, 2-aminophenol(L^1)/2-aminobenzoic acid (L^2) and-aminothiazole (L^3). Their Cu(II) complexes have also been synthesized and characterized on the basis of ^{1}H NMR, IR, UV–Vis spectra, elemental analyses, molar conductivity, ESR, electrochemical behaviour and thermal analyses. The antimicrobial activities (MIC values) of the ligands, copper complexes and standard drugs have been evaluated using the serial dilution technique against the bacterial species *Staphylococcus aureus, Escherichia coli, Klebsiella pneumoniae, Proteus vulgaris* and *Pseudomonas aeruginosa* and fungal species *Aspergillus niger, Rhizopus stolonifer, Aspergillus flavus, Rhizoctonia bataicola* and *Candida albicans*. The anti-inflammatory and SOD activities of the investigated compounds are also promising and allow the selection of a lead compound for further biological studies.

1. Introduction

Flavones occupy a special place in the realm of natural and synthetic organic chemistry owing to their useful biological activities such as anti-oxidant (Rice-Evans, 2001), Anxiolytic (De Almeida et al., 2009), anti-cancer (Liu et al., 1992), analgesic (Shin et al., 1999), and anti-microbial (Sohel et al., 2006). During the past few years various methods have been reported for the synthesis of flavones (Diana, 2000; Kumar and Perumal, 2007; Ballesteros et al., 1995).

The copper is an essential micronutrient for feeding and a cofactor of several enzymes involved in oxidative metabolism like β-hydroxylases, quercetinase, ceruloplasmine, cytochromoxidase, monoaminoxidase, superoxydismutase, ascorbic acid oxidase and tyrosinase (Berdanier et al., 1999; Brill et al., 1964 and Frieden et al., 1965). The catalytical role of these enzymes is a two-step process, i.e., the reduction of Cu^{2+}

* Corresponding author. Tel.: +91 09629474150; fax: +91 4562230414.
E-mail address: chem_joseph@yahoo.co.in (J. Joseph).
Peer review under responsibility of King Saud University.

ELSEVIER Production and hosting by Elsevier

http://dx.doi.org/10.1016/j.arabjc.2011.06.027
1878-5352

ion to Cu^+ and the fixation of molecular oxygen (Halfen et al., 1996). The copper(II) complexes of multidentate Schiff base ligands have played a vital role in the development of coordination chemistry (Chiari et al., 2001; Swearingen and West, 2001).

A range of monocarboxylic acids are known to have a variety of pharmacological effects. Salicylic acid and its derivatives, for example, have been shown to possess anti-inflammatory and antitumour activity (Sorenson, 1976). Upon coordination to a suitable metal centre, the biologically active carboxylic acids often become more effective and desirable drugs (Sorenson, 1989). The carboxylate group is an important class of ligands in inorganic and bioinorganic chemistry, metal complexes containing monocarboxylic acids are well known, and the publication of many structurally characterised examples of this class of compound has demonstrated its versatility as an inner-sphere ligand (Mehrotra and Bohra, 1983).

As part of our continuous investigations, we report here the synthesis, structural aspects and biological studies of copper(II) complexes of the above said Schiff base ligands. The anti-inflammatory activity of the ligands and their complexes has also been studied.

2. Experimental

Analytical grade chemicals commercially available purchased from BDH, Aldrich, Fischer etc were used for synthesis and solvents were purified by standard methods.

Micro analytical data and FAB Mass spectra of the compounds were recorded at the Regional Sophisticated Instrumentation Center, Central Drug Research Institute (RSIC, CDRI), Lucknow. The amount of copper present in the copper complexes was estimated using AAS. The NMR spectra of the ligands were recorded using TMS as internal standard. Chemical shifts (δ) are expressed in units of parts per million relative to TMS. The FAB mass spectrum of the ligands and their complexes were recorded on a JEOL SX 102/DA-6000 mass spectrometer/data system using argon/xenon (6 kV, 10 mA) as the FAB gas. The accelerating voltage was 10 kV and the spectra were recorded at room temperature using m-nitrobenzylalcohol (NBA) as the matrix. Molar conductance of the copper complexes was measured in DMSO solution using a coronation digital conductivity metre. The IR spectra of the ligands and their copper complexes were recorded on a Perkin-Elmer 783 spectrophotometer in 4000–200 cm^{-1} range using KBr disc. Electronic spectra were recorded with a Systronics 2201 Double beam UV–Vis, spectrophotometer in the 200–1100 nm region. The magnetic susceptibility values were calculated using the relation $\mu_{eff} = 2.83\ (\chi_m.T)$. The diamagnetic corrections were made by Pascal's constant and $Hg[Co(SCN)_4]$ was used as a calibrant. The ESR spectra of the copper complexes were recorded at 300 and 77 K on a Varian E112 X-band spectrometer. Cyclic voltammetric measurements were performed using a glassy carbon working electrode, Pt wire auxiliary electrode and an Ag/AgCl reference electrode. Tetrabutylammoniumperchlorate (TBAP) was used as the supporting electrolyte. All solutions were purged with N_2 for 30 min prior to each set of experiments. The computer controlled X-ray diffractometer system JEOL JDX 8030 was used to record powder data for the copper complexes, at the Central Electrochemical Research Institute, Karaikudi.

2.1. Preparation of Ligand (L^1–L^3)

Equimolar amount of 3-hydroxyflavone and o-aminophenol (L^1)/o-aminobenzoic acid (L^2)/o-aminothiazole (L^3) was dissolved in ethanol (40 mL). Acetic acid (1.0 mL) was added to this solution. The solution was stirred for 3 h and the precipitate was formed. The precipitate was filtered and washed with water and ethanol.

L^1: Yield: 60%. Anal. Calcd for $C_{21}H_{15}NO_3$: C, 76.58; H, 4.59; N, 4.25. Found: C, 76.64; H, 4.62; N, 4.28. FAB mass spectrometry (FAB-MS), m/z 330 [M + 1]. ^{1}H-NMR (400 MHz, $CDCl_3$) δ: 6.6–7.8 (13H, m, Ar-H) and 11.2 and 10.8 (2H, s, O–H, D_2O exchangeable, 3-hydroxyflavone and o-aminophenol moities). ^{13}C-NMR (400 MHz, $CDCl_3$, ppm): 150.8 (C-2), 140.6 (C-3), 153.8 (C-4), 112.8(C-5), 145.6 (C-6), 124.4 (C-7), 126.9 (C-8), 156.6 (C-9), 118.8 (C-10), 133.6 (C-1′), 124.3 (C-2′, 6′), 126.5 (C-3′, 5′), 126.4 (C-4′), 130.6 (C-1″), 115.2 (C-2″), 120.6 (C-3″), 119.2 (C-4″), 126.2 (C-5″) and 140.8 (C-6″).

L^2: Yield: 65%. Anal. Calcd for $C_{22}H_{15}NO_4$: C, 73.94; H, 4.23; N, 3.91. Found: C, 73.98; H, 4.26; N, 3.98. FAB mass spectrometry (FAB-MS), m/z 358 [M + 1]. ^{1}H-NMR (400 MHz, $CDCl_3$) δ: 6.7–7.9 (12H, m, Ar-H), 11.6 and 10.4 (2H, ^{13}C-NMR (400 MHz, $CDCl_3$, ppm): 149.4 (C-2), 110.2 (C-3), 154.5 (C═N), 115.6 (C-5), 146.4 (C-6), 122.8 (C-7), 126.4 (C-8), 152.6 (C-9), 119.9 (C-10), 132.5 (C-1′), 125.4 (C-2′, 6′), 127.6 (C-3′, 5′), 126.5 (C-4′), 148.6 (C-1″), 113.4 (C-2″), 132.6 (C-3″), 116.5 (C-4″), 128.9 (C-5″), 140.8 (C-6″) and 168.2 (COOH).

L^3: Yield: 62%. Anal. Calcd for $C_{18}H_{12}N_2O_2S$: C, 67.49; H, 3.78; N, 8.75. Found: C, 67.42; H, 3.72; N, 8.69. Fast atom bombardment mass spectrometry (FAB-MS), m/z 322 [M + 1]. ^{1}H-NMR (400 MHz, $CDCl_3$) δ: 5.9–7.9 (13H, m,Ar-H), 12.9 and 10.8 (2H, s, S–H & O-H, D_2O exchangeable). ^{13}C-NMR (400 MHz, $CDCl_3$): 149.4 (C-2), 110.2 (C-3), 154.5 (C═N), 115.6 (C-5), 147.4 (C-6), 122.6 (C-7), 126.9 (C-8), 154.6 (C-9), 121.9 (C-10), 132.5 (C-1′), 125.4 (C-2′, 6′), 127.6 (C-3′, 5′), 126.5 (C-4′), 158.6 (C-11), 103.4 (C-12) and 148.9 (C-13).

2.1.1. Preparation of copper complexes of Ligands (L^1–L^3)

The ligand (s) (0.05 mM) and copper acetate (0.05 mM) were dissolved in acetone (20 mL). Under stirring, triethylamine (0.075 mM) was then dropped to the mixture with caution. After stirring for 4 h at room temperature, the precipitate was separated, purified by washing several times with acetone and dried in vacuum.

Complex of L^1: Yield: 74%. Anal. Calcd for $CuC_{21}H_{17}NO_4$: C, 61.36; H, 4.17; N, 3.41, Cu, 15.47. Found: C, 61.31; H, 4.15; N, 3.36; Cu, 15.43. FAB mass spectrometry (FAB-MS), m/z 411 [M + 1]. μ_{eff} (BM) = 1.92; Λ_m (mhocm^2 mol^{-1}) = 24.

Complex of L^2: Yield: 79%. Anal. Calcd for $CuC_{22}H_{17}NO_5$: C, 60.18; H, 3.91; N, 3.19, Cu, 14.49. Found: C, 60.14; H, 3.86; N, 3.15; Cu, 14.43. FAB mass spectrometry (FAB-MS), m/z [M + 1]. μ_{eff} (BM) = 2.06; Λ_m (mhocm^2 mol^{-1}) = 29.

Complex of L^3: Yield: 76%. Anal. Calcd for $CuC_{20}H_{15}N_2O_4S$: C, 54.22; H, 3.42; N, 6.33; Cu, 14.36. Found: C, 74.62; H, 3.35; N, 6.29; Cu, 14.31. FAB mass spectrometry (FAB-MS), m/z 443 [M + 1]. μ_{eff} (BM) = 1.98; Λ_m (mhocm^2 mol^{-1}) = 8.

2.2. Biological studies

2.2.1. Antimicrobial activity

The in vitro antimicrobial activities of the investigated compounds were tested against the bacterial species, *Staphylococcus aureus, Escherichia coli, Klebsiella pneumoniae, Proteus vulgaris* and *Pseudomonas aeruginosa* and fungal species, *Aspergillus niger, Rhizopus stolonifer, Aspergillus flavus, Rhizoctonia bataicola* and *Candida albicans*. One day prior to the experiment, the bacterial and fungal cultures were inoculated in broth (inoculation medium) and incubated overnight at 37 °C. Inoculation medium containing 24 h grown culture was added aseptically to the nutrient medium and mixed thoroughly to get the uniform distribution. This solution was poured (25 mL in each dish) into petri dishes and then allowed to attain room temperature. Wells (6 mm in diameter) were cut in the agar plates using proper sterile tubes. Then, fill wells were filled up to the surface of agar with 0.1 mL of the test compounds dissolved in DMSO (200 μM/mL). The plates were allowed to stand for an hour in order to facilitate the diffusion of the drug solution. Then the plates were incubated at 37 °C for 24 h for bacteria and 48 h for fungi and the diameter of the inhibition zones were read. Minimum inhibitory concentrations (MICs) were determined by using the serial dilution method. The lowest concentration (μg/mL) of compound, which inhibits the growth of bacteria after 24 h incubation at 37 °C, and of fungi after 48 h incubation at 37 °C was taken as the MIC.

2.2.2. SOD activity

In vitro SOD activity was measured using alkaline DMSO as a source of superoxide radical (O_2^-) and nitrobluetetrazolium (NBT) as O_2^- scavenger. In general, 400 μL sample to be assayed was added to a solution containing 2.1 mL of 0.2 M potassium phosphate buffer (pH 8.6) and 1 mL of 56 μM NBT. The tubes were kept in ice for 15 min and then 1.5 mL of alkaline DMSO solution was added while stirring. A unit of superoxide dismutase [SOD] activity is the concentration of complex or enzyme, which causes 50% inhibition of alkaline dimethylsulfoxide (DMSO) mediated reduction of nitrobluetetrazolium chloride (NBT) (absorbance was then monitored at 540 nm).

2.2.3. Anti-inflammatory studies

The anti-inflammatory activity of copper complexes was determined by using the carrageenan-induced paw oedema method. Groups of five rats with masses of 180–220 g were used. A suspension containing single dose of 0.01 mmol/kg body mass per 1 mL of the copper complexes, suspended in isotonic sterile saline water, with few drops of Tween 80 and ground in a mortar to suspend, was given IP at the same time as the phlogistic agent, carrageenin. Carrageenin (2%) in 0.1 mL of isotonic sterile saline water was injected intradermally into the right foot pad, the left paw serving as control. Indomethacin, reference drug, was administered IP, simultaneous with the administration of the phlogistic agent. Controls received the liquid vehicle. These animals were euthanized 3.5 h after carrageenin injection. Both hind paws were severed above the ankle joint and immediately massed with a very sensitive analytical balance. The experiment was repeated for each compound with a second group of five animals. The difference between masses of the injected and uninjected paws was calculated for each animal. The change in paw mass was compared with that for control animals injected with isotonic sterile saline water and expressed as percent inhibition of oedema, CPE% values in Table 6.

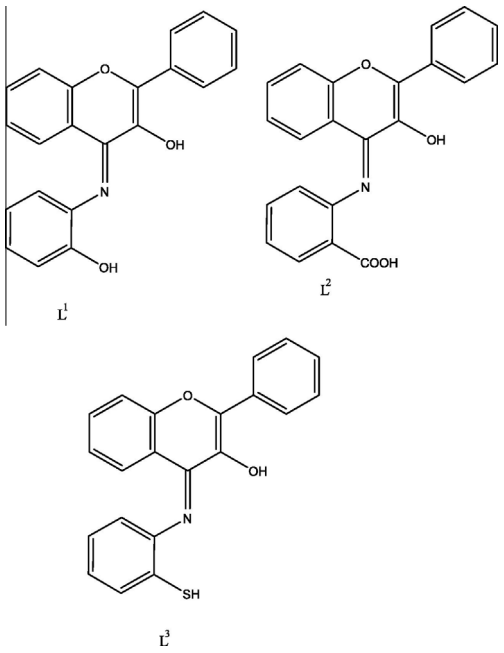

Figure 1 The proposed structures of ligands (L^1-L^3).

3. Results and discussion

The Schiff bases (Fig. 1) are prepared as described in the experimental part, crystallized and dried under vacuum and subjected to elemental analyses. The results obtained are in good agreement with those calculated for the suggested formulae and the melting points are sharp indicating the purity of the prepared Schiff bases. All complexes were decomposed above 280 °C indicating their thermal stability.

3.1. Molar conductance

The molar conductance data for the copper complexes measured in DMSO solution for the 0.001 M solutions are given in Section 2. The values of the complexes fall in the range of 8–29 Ω^{-1} cm^2 mol^{-1}, which is the expected range of 1–35 Ω^{-1} cm^2 mol^{-1} for the complexes to behave as non-electrolytes (Geary, 1971). Thus, the complexes have non-electrolytic nature as evidenced by the involvement of the acetate group in coordination. This result was confirmed from the chemical analysis of CH_3COO^- ion not precipitated by addition of $FeCl_3$. The complexes did not show electrolytic properties.

Table 1 Electronic spectral data of ligands and their copper complexes.

S. no.	Compound	Solvent	Absorption (nm)	Band assignment	Geometry
1	L^1	DMSO	215	INCT	–
			312	INCT	
2	L^2	DMSO	232	INCT	–
			336	INCT	
3	L^3	DMSO	248	INCT	–
			342	INCT	
4	$[CuL^1(H_2O)]$	DMSO	228	INCT	
			342	INCT	
			578	$^2B_{1g} \rightarrow {}^2A_{1g}$	Square planar
5	$[CuL^2(H_2O)]$	DMSO	248	INCT	
			342	INCT	
			530	$^2B_{1g} \rightarrow {}^2A_{1g}$	Square planar
6	$[CuL^3(H_2O)]$	DMSO	254	INCT	
			348	INCT	
			572	$^2B_{1g} \rightarrow {}^2A_{1g}$	Square planar

3.2. IR spectra

In order to study the binding mode of the Schiff base to the metal in the complexes, the IR spectrum of the free ligand was compared with the spectra of the complexes. The IR spectrum of the ligands shows a ν(C═N) peak in the region 1645–1632 cm^{-1}. The IR spectra of all complexes show ν(C═N) bands at 1629–1590 cm^{-1} (Bansod et al., 2007) and it is found that the ν(C═N) bands in the complexes are shifted to lower energy regions compared to the free ligands. The shift of this band towards energy side is probably caused by an increase in the C═N bond order due to the coordination of the nitrogen with the copper atom.

However, the spectra of complexes show two characteristic bands at 1630–1602 and 1404–1344 cm^{-1} attributed to υ_{asy}(-COO^-) and $\upsilon_{sy.}$(COO^-), respectively, indicating the participation of the carboxylate oxygen atom in the complexes. The mode of coordination of the carboxylate group has often been deduced from the magnitude of the observed separation between the υ_{asy}(COO^-) and $\upsilon_{sy.}$(COO^-), the separation value (A) between υ_{asy}(COO^-) and $\upsilon_{sy.}$(COO^-) in metal complexes was more than 200 cm^{-1} (260–216 cm^{-1}) which suggests the coordination of the carboxylate group in copper complexes of the ligands in a monodentate fashion (Nakamoto, 1988). The Schiff base ligands display a band around 844 cm^{-1} ascribed to υ C–S (Sandipan Sarkar et al., 2009) which shifts to lower frequencies in their spectra of copper complexes in the region 838–832 cm^{-1}, respectively, suggesting the coordination of copper ions through the sulfur atom of the thioazole moiety. The band at 3466 cm^{-1} for υ(OH) in the free ligand disappeared on complexation, indicating coordination through a deprotonated oxygen.

The band observed in the region 1534–1526 cm^{-1} is due to the $\nu_{C=C}$ stretching of the aromatic ring system. In all the copper-Schiff base complexes, most of the band shifts observed in the wave number region 1142–980 cm^{-1} are in agreement with the structural changes observed in the molecular carbon skeleton after complexation, which cause some changes in the (C–C) bond lengths. Conclusive evidence of the bonding is also shown by the observation that new bands in the spectra of all copper complexes appear in the low frequency regions at 550–516, 504–498 and 486–448 cm^1 characteristic to υ(M–O), υ(M–N) and υ(M–S) stretching vibrations, respectively, that are not observed in the spectra of free ligands (Anacona et al., 2009). The IR bands at 810–854 and 784–799 cm^{-1}, $\upsilon(H_2O)$ of coordinated water, is an indication of the binding of the water molecules to the metal ions.

3.3. Electronic spectra

The electronic spectra of the Schiff base ligands and their copper complexes in DMSO were recorded at room temperature and the band positions of the absorption maxima; band assignments and the proposed geometry are shown in Table 1. The electronic spectra of the ligands and their complexes were recorded in DMSO as a solvent. The absorption spectrum for L^1 shows band at 225 and 312 nm. These bands can be attributed to n–$\pi^*$and π–π^* transitions within the Schiff base molecule. The electronic spectrum of the corresponding $[CuL^1(H_2O)]$ complex in DMSO reveals a broad band at 558 nm assignable to $^2B_{1g}\rightarrow{}^2A_{1g}$ transition (Chandra and Gupta, 2005) which is characteristic of square planar environment around the copper(II) ion. Similar spectral features were assigned for other complexes.

The electronic spectra of all the complexes exhibit bands in the regions 200–225, 272–332 and 362–390 nm, which may be due to the π–π^* transition of the benzenoid/or n–π^* (COO), π–π^* transition of the >C═N– chromophore and n–π^* transition of the >C═N– chromophore, coupled with the secondary band of the benzene ring, respectively. Further, there were a few sharp bands observed in the region 233–257 nm in the spectra of the complexes, which could be assigned as charge transfer bands.

3.4. NMR spectra

The ^1H and ^{13}C-NMR spectrum of ligands were recorded in $CDCl_3$ and are given in Section 2. All the protons were found as to be in their expected region (Li et al., 2008). The conclu-

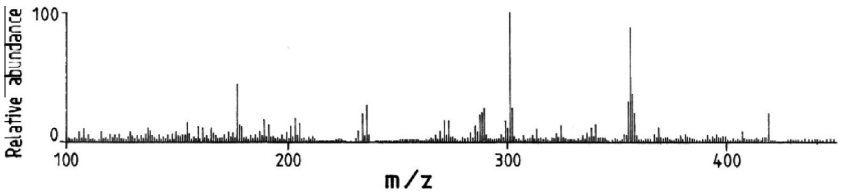

Figure 2 FAB mass spectrum of Ligand (L^1).

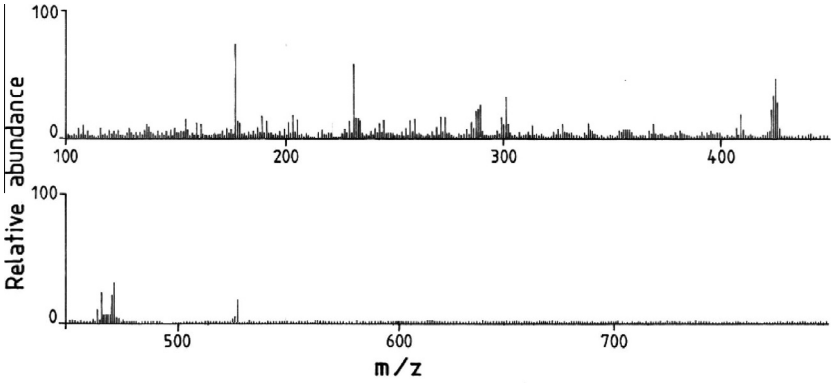

Figure 3 FAB mass spectrum of [$CuL^1(H_2O)$] complex.

sions drawn from these studies lend further support to the mode of bonding discussed in their IR spectra. The number of protons calculated from the integration curves and those obtained from the values of the expected CHN analyses agree with each other. The ^1H and ^{13}C-NMR spectra of the copper complexes could not be obtained due to their paramagnetic nature.

3.5. FAB mass spectra

Mass spectra provide a vital clue for elucidating the structure of the compounds. The mass spectra of the ligand (L^1) and its copper complex [$CuL^1(H_2O)$] were recorded and their stoichiometric compositions were compared. The intensity of these peaks reflects the stability and abundance of the ions (Hamming and Foster, 1972). The molecular ion peak for the ligand (L^1) is observed at 424m/z (Fig. 2) whereas its copper complex shows the molecular ion peak at 515m/z (Fig. 3), which confirms the stoichiometry of the metal complexes to be [$CuL^1(H_2O)$] type. Elemental analysis values are in close agreement with the values calculated from molecular formula assigned to these complexes, which is further supported by the FAB-mass studies of respective complexes. Similar mass spectral features were assigned for other ligands and their copper complexes.

3.6. ESR spectra

The ESR spectrum of the [$CuL^1(H_2O)$] complex was recorded in DMSO at 300 and 77 K. The spectrum at 300 K shows one intense absorption band at high field, which is isotropic due to the tumbling motion of the molecules. However, this complex in the frozen state (77 K) shows four well resolved peaks with low intensities in the low field region and one intense peak in the high field region. The magnetic susceptibility value reveals that the copper complex has a magnetic moment of 1.92 B.M corresponding to one unpaired electron, indicating that the complex is mononuclear in nature. This fact was also evident from the absence of half field signal, observed in the spectrum at 1600 G due to the $\Delta m_s = \pm 2$ transitions, ruling out any Cu–Cu interaction (Gaballa et al., 2007). The ESR spectral data are given in Table 2.

The f value for cu, Zn SOD is 160 cm indicating a tetrahedral distortion from square planar geometry and is one of the features that enhances the catalytic activity of the enzyme. From the above EPR data, the f values for copper complexes were determined to be in the range of 142–158 cm. Therefore, our synthesized copper complexes exhibiting appreciable square planar distortion are expected to show high SOD like activity. Molecular orbital coefficients α^2 (in-plane σ-bonding),

Table 2 ESR spectral data of the copper complexes.

Complex	$g_{\|\|}$	$g_\perp$	g_{iso}	$A_{\|\|}$	$A_\perp$	$K_{\|\|}$	$K_\perp$	α^2	β^2	γ^2	$f(g_{\|\|}/A_{\|\|})$
[$CuL^1(H_2O)$] at 300 K			2.06								
[$CuL^1(H_2O)$] at 77 K	2.23	2.06	–	150	44	0.90	0.52	0.76	1.34	0.738	148
[$CuL^2(H_2O)$] at 300 K			2.10								
[$CuL^2(H_2O)$] at 77 K	2.21	2.08	–	142	56	0.84	0.48	0.72	1.43	0.726	155
[$CuL^3(H_2O)$] at 300 K			2.12								
[$CuL^3(H_2O)$] at 77 K	2.24	2.07	–	154	58	0.75	0.46	0.80	1.32	0.841	145

β^2 (in-plane π-bonding) and γ^2 (out-plane π-bonding) were calculated using Eqs. (1)–(3).

$$\alpha^2 = -(A_{\parallel}/0.036) + (g_{\parallel} - 2.0036) + 3/7(g_{\perp} - 2.0036) + 0.04 \quad (1)$$

$$\beta^2 = (g_{\parallel} - 2.0036)E/ - 8\lambda\alpha^2 \quad (2)$$

$$\gamma^2 = (g - 2.0036)E/ - 2\lambda\alpha^2 \quad (3)$$

The α^2 value of 0.5 indicates complete covalent bonding, while that of 1.0 suggests complete ionic bonding. The observed value of 0.76 for the present complex indicates that the copper complex has some covalent character. The observed β^2 and γ^2 values of 1.34 and 0.738 indicate that there is interaction in the out-of-plane π-bonding, whereas the in-plane π-bonding is predominantly ionic. Significant information about the nature of bonding in the Cu(II) complex can be derived from the relative magnitudes of $K_{\parallel}$ and $K_{\perp}$.

$$K_{\parallel} = \alpha^2\beta^2 \quad (4)$$

$$K_{\perp} = \alpha^2\gamma^2 \quad (5)$$

For the present complex, the observed order: $K_{\parallel}(0.90) > K_{\perp}(0.52)$ implies a greater contribution from out-of plane π-bonding than from in in-plane π-bonding in metal–ligand π bonding.

3.7. Cyclic voltammetry

Cyclic voltammetry is the most versatile electroanalytical technique for the study of the electroactive species. The important parameters of a cyclic voltammogram are the magnitudes of the anodic peak current (ipa), cathodic peak current (ipc), anodic peak potential (Epa) and cathodic peak potential (Epc). The copper(II) complexes in the DMSO solution undergo one electron reduction and also one electron oxidation to form monovalent and trivalent metal species. The electrochemical behaviours of the Schiff base Cu(II) complexes in DMSO (0.1 M of TBAP as supporting electrolyte (scan rate 100 mVs^{-1}) at 300 K were examined. Table 3 summarizes the potentials and their assignments, which mainly depend on the geometry and environment around the copper ion (i.e., ligand core).

All copper complexes show well-defined redox couple corresponding to copper(II/I). The cathodic peak appearing in the negative potential of 658–768 mV range corresponds to the reduction of copper(II) and the corresponding anodic peak also appears in the negative potential of 658–526 mV which corresponds to the oxidation of copper(I). The measured ΔEp values (116–158 mV) clearly indicate that these redox couples are quasi-reversible in nature. The i_{pa}/i_{pc} falls at ca. 0.9–1.1, clearly confirming one electron transfer in this redox process.

The cyclic voltammogram of the $[CuL^1(H_2O)]$ complex in the DMSO solution at 300 K in the potential range +0.4 to −0.8 V at scan rate 0.1 $V\,s^{-1}$ was recorded (Fig. 4). It shows a well defined redox process corresponding to the formation of the quasi-reversible Cu(II)/Cu(I) couple. The anodic peak at Epa = 0.065 mV versus Ag/AgCl and the associated cathodic peak at Epc = 0.076 mV correspond to the Cu(II)/Cu(I) couple. The $[CuL^1(OAc)]$ complex exhibits a quasi-reversible behaviour.

The cyclic voltammogram of the $[CuL^2(H_2O)]$ and $[CuL^3(H_2O)]$ complexes in the DMSO solution at 300 K are shown in Figs. 4 and 5. On comparing the cyclic voltammograms, we observed that the variation in oxidation and reduction potential may be due to distortion in the geometry of the complexes which arises due to different donor atoms coordinated to the copper ion. It is concluded that the present ligand systems stabilize the unusual oxidation states of copper ion during electrolysis. Similar electrochemical behaviour was observed and assigned for other complexes.

3.8. Thermogravimetric analyses

The thermal decomposition studies of the complexes were carried in the temperature range 30–600 °C with a sample heating rate 5 °C/min in a static nitrogen atmosphere. All the complexes undergo first step decomposition with weight loss between 220 and 250 °C due to loss of the one coordinated water molecule. The complexes show the second step decomposition between 390 and 420 °C due to removal of half part of the ligand. Finally the complexes undergo decomposition between 500 and 530 °C due to loss of the remaining part of ligand. The final residue was analysed by IR spectra and identified as CuO which corresponds to the calculated value. These features support the formulae $[CuL^1(H_2O)]$, $[CuL^2(H_2O)]$ and $[CuL^3(H_2O)]$, assigned to the complexes.

3.9. XRD

The crystallite size of the complex was calculated from the Scherre's formula:

$$d_{XRD} = 0.9\lambda/\beta\cos\theta,$$

where λ is the wavelength, β is the full-width half maximum of the characteristic peak and θ is the diffraction angle for the *hkl* plane.

From the observed d_{XRD} patterns, the average crystallite sizes for the copolymer $[CuL^1(H_2O)]$, $[CuL^2(H_2O)]$ and $[CuL^3(H_2O)]$ complexes are found to be 75, 84 and 62 nm, respectively.

Table 3 Cyclic voltammetric data of copper complexes.

Complex	E_{pa}	E_{pc}	ΔE_p	Potential assignment
$[CuL^1(H_2O)]$	−0.658	−0.766	108	Cu(II)/Cu(I)
	0.432	–	–	Cu(II)/Cu(III)
$[CuL^2(H_2O)]$	0.33	−0.198	154	Cu(II)/Cu(I)
	0.632	–		Cu(II)/Cu(III)
$[CuL^3(H_2O)]$	0.316	−0.264	140	Cu(II)/Cu(I)
	0.764	–	–	Cu(II)/Cu(III)

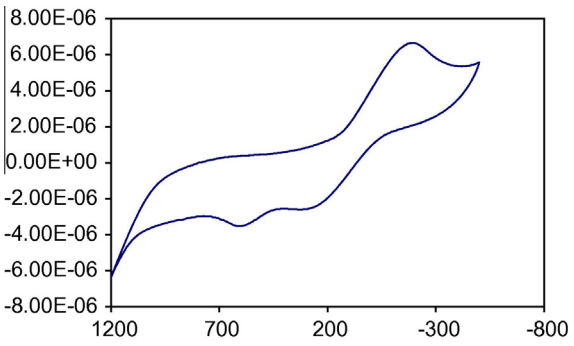

Figure 4 Cyclic voltammogram of $[CuL^2(H_2O)]$ complex.

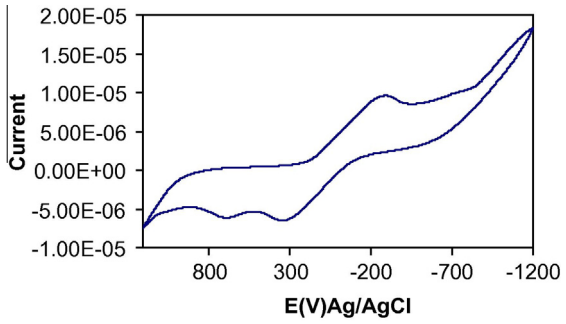

Figure 5 Cyclic voltammogram of $[CuL^3(H_2O)]$ complex.

3.10. Antimicrobial activity

To contribute in the field of bioinorganic chemistry, consequently, the compounds synthesized have been evaluated for their antibacterial, antifungal, DNA binding studies. The antibacterial and antifungal tests were carried out using the serial dilution method.

Table 6 Superoxide dismutase activity of some copper(II) complexes.

S. no.	Complex	IC_{50} (mol dm^{-1})
1	$[CuL^1(H_2O)]$	80
2	$[CuL^2(H_2O)]$	68
3	$[CuL^3(H_2O)]$	94

The in vitro antimicrobial activities of the investigated compounds were tested against the bacterial species *S. aureus*, *E. coli*, *K. pneumaniae*, *P.* vulgaris and *P.* aeruginosa and fungal species *A. niger*, *R. stolonifer*, *A. flavus*, *R.* bataicola and *C. albicans*. The minimum inhibitory concentration (MIC) values of the compounds are summarized in Tables 4 and 5. A comparative study of the ligands and their complexes (MIC values) indicates that complexes exhibit higher antimicrobial activity than the free ligands. In this study, the antimicrobial activity of the ligands may be due to the heteroaromatic residues. Compounds containing >C═N group have enhanced antimicrobial activity than >C═C< group. The growth of certain microorganisms takes place even in the absence of O_2.

The enhanced activity of the complexes can be explained on the basis of the Overtone's concept (Anjaneyula and Rao, 1986) and Tweedy's Chelation theory (Dharamaraj et al., 2001). Chelation can considerably reduce the polarity of the metal ion, which in turn increases the lipophilic character of the chelate. Thus, the interaction between metal ion and the lipid is favoured. This may lead to the breakdown of the permeability barrier of the cell, resulting in interference with the normal cell processes. If the geometry and charge distribution around the molecule are incompatible with the geometry and charge distribution around the pores of the bacterial cell wall,

Table 4 Minimum inhibitory of concentration of the synthesized compounds against growth of bacteria (μg/mL).

S. no.	Compound	*E. coli*	*K. pneumoniae*	*P. vulgaris*	*P. aeruginosa*	*S. aureus*
1	L^1	60	64	66	66	72
2	L^2	24	26	20	16	28
3	L^3	28	36	26	32	30
4	$[CuL^1(H_2O)]$	34	38	32	28	42
5	$[CuL^2(H_2O)]$	26	28	30	26	48
6	$[CuL^3(H_2O)]$	52	54	58	60	63
7	Streptomycin	10	15	6	12	4

Table 5 Minimum inhibition of concentration of the synthesized compounds against growth of fungi (μg/mL).

S. no.	Compound	*A. niger*	*R. stolonifer*	*A. flavus*	*R. bataicola*	*C. albicans*
1	L^1	60	66	72	80	50
2	L^2	19	20	20	25	22
3	L^3	24	28	28	34	30
4	$[CuL^1(H_2O)]$	28	30	34	38	32
5	$[CuL^2(H_2O)]$	32	26	46	36	38
6	$[CuL^3(H_2O)]$	52	55	68	80	50
7	Nystatin	10	16	8	14	12

Table 7 Reduction of inflammation by prepared compounds and indomethacin (reference drug) on carrageenin induced rat paw oedema (CPE%) compared with vehicle treated control rats.

S. no.	Compounds	Dose (mmol/kg BM[a])	CPE%[b]
1	$[CuL^1(H_2O)]$	0.01	26.5[d]
2	$[CuL^2(H_2O)]$	0.01	64.0[d]
3	$[CuL^3(H_2O)]$	0.01	32.6[c]
Control	Indomethacin	0.01	48.3[d]

(For comparison with controls, Student's *t*-test).
[a] BM = body mass.
[b] CPE = Carrageenin Paw Oedema.
[c] $p < 0.01$.
[d] $p < 0.05$.

penetration through the wall by the toxic agent cannot take place and this will prevent the toxic reaction with in the pores.

Chelation is not the only criterion for antibacterial activity. Some important factors that contribute to the activity are nature of the metal ion, nature of the ligand, coordinating sites, geometry of the complex, concentration, hydrophilicity, and lipophilicity. Certainly, steric, and pharmokinetic factors also play a decisive role in deciding the potency of an antimicrobial agent. The higher toxicity of the metal complex can be attributed to the effect of metal ion on the normal cell processes. The widespread interaction of metal ions with cellular compounds is due to the fact that all these structures contain a variety of functional groups that can act as metal binding ligands. The problem is how to obtain those interactions in cells and organisms where the non-polar membrane exists to hinder the movement of charged metal ions into the cell, where myriad of metal binding sites exists to compete for the metal ion, and where specificity of cellular interaction must occur in order to obtain therapeutic value.

Apart from this, the mode of action of these compounds may also invoke the hydrogen bond though the imine C═N group with the active centres and thus interfere with normal cell processes. Presence of lyphophilic and polar substituents is expected to enhance antimicrobial activities. Heterocyclic ligands with multifunctionality have greater chance of interaction either with nucleoside bases (even after complexation with metal ion) or with biologically essential metal ions present in the biosystem which can be promising candidates as bactericides since they always look to enact especially with some enzymatic functional groups, to achieve higher coordination number. Thus, the antibacterial property of metal complexes cannot be ascribed to chelation alone but it is an intricate blend of all the above contributions.

3.11. SOD activity

A great deal of interest has been shown in the development of therapeutic SOD mimetics for the scavenging of superoxide ($O_2^{\cdot-}$) which is a precursor to reactive oxygen and nitrogen species (RONS) known to contribute to oxidative stress. The SOD mimetic activities of the copper(II) complexes were determined and compiled in Table 6. In the present study, $[CuL^3(H_2O)]$ has higher SOD activity as compared to other complexes. A greater interaction between superoxide ion and Cu(II) complex is induced due to the stronger axial bond, which results in an increased catalytic activity. In addition azomethine ligands containing electron withdrawing substituent stabilizes the Cu(I) complex formed during superoxide dismutation reaction which further reacts with superoxide ion to give hydrogen peroxide. The distorted geometry of these complexes may favour the geometrical change, which is essential for the catalysis as the geometry of copper in the SOD enzyme also changes from distorted square planar geometry. The difference in reactivities of the synthesized complexes may be attributed to the coordination environment and the redox potential of the couple Cu^+/Cu^{++} in copper(II) complexes during the catalytic cycle. It has been reported that the redox potential of copper(II) ions is affected by the coordination structure of copper(II) complexes (Díaz et al., 2009) (see Table 7).

3.12. Anti-inflammatory activity

The reference drug, indomethacin, is a non-steroidal anti-inflammatory drug, which is used for the treatment of a broad spectrum of inflammation related diseases suggested to be due to inhibition of prostaglandin syntheses. The initial phase is attributed to the release of histamine and serotonin. The oedema maintained between the first and the second phase is due to kinin like substances (Lazzaroni and Bianchi Porro, 2004). The second phase is said to be promoted by prostaglandin like substances. It has been reported that the second phase of oedema is sensitive to drugs like hydrocortisone, phenylbutazone and indomethacin. The results show that the copper complex which has higher activity than other complexes is due to the high diffusion of the copper complex.

4. Conclusion

In conclusion, the synthesized 3-hydroxyflavone derivatives can be potentially useful for anti-inflammatory agents that can prompt future researchers to synthesise a series of 3-hydroxyflavone derivatives which contains wide variety of substituents with the aim of obtaining novel heterocyclic (biosensitive) compounds with enhanced activity.

Acknowledgements

The authors express their heartfelt thanks to the Chairman, Noorul Islam Centre for Higher Education, Kumaracoil for providing research facilities. JJ and KN express their gratitude to the DST, New Delhi for financial assistance under the INSPIRE fellowship (IF 10544).

References

Anacona, J.R., Daniel, Lorono, Mary, azocar, Reinaldo, Atencio, 2009. J. Coord. Chem. 62, 951–957.
Anjaneyula, Y., Rao, R.P., 1986. Synth. React. Inorg. Met. Org. Chem. 16, 257–272.
Ballesteros, J.F., Sanz, M.J., Ubeda, A., Miranda, M.A., Iborra, S., Paya, M., Alcaraz, M.J., 1995. J. Med. Chem. 38 (14), 2794–2797.
Bansod, A.D., Mahale, R.G., Aswar, A.S., 2007. Russ. J. Inorg. Chem. 52, 879–883.

Berdanier, C.D., Groff, J.L., Gropper, S.S., 1999. Advanced Nutrition and Human Metabolism, 3rd ed. Wordsworth/Thompson Learning, Belmont, CA.
Brill, A.S., Martin, R.B., Williams, R.J.P., 1964. Electronic Aspects of Biochemistry. Academic Press Inc., New York.
Chandra, S., Gupta, L.K., 2005. Spectrochim. Acta 61A, 269–275.
Chiari, A.S., Daon, P.E., Hoffman, B.M., Ibers, J.A., 2001. Angew Chem. Int. Ed. Engl. 40, 244.
De Almeida, E.R., Xavier, H.S., Chaves, T.M., Couto, G.B.C., Aragao-Neto, A.C., Silva, A.R., Da Silva, L.L.S., 2009. Int. J. Appl. Res.. Natural Products 2 (4), 44–51.
Dharamaraj, N., Viswanathamurthi, P., Natarajan, K., 2001. Transition Met. Chem. 26, 105–109.
Diana, C.G.A.P., 2000. Artur MSS and Jose ASC. New J. Chem. 24, 85–92.
Díaz, Alicia M., Villalonga, Reynaldo., Cao, Roberto, 2009. J. Coord. Chem. 62, 100–107.
Frieden, E., Osaki, S., Kobayashi, H., 1965. J. Gen. Physiol. 49, 213.
Gaballa, A.S., Asker, M.S., Barakat, A.S., Teleb, S.M., 2007. Spectrochim. Acta A. 67, 114–121.
Geary, W.J., 1971. Coord. Chem. Rev. 7, 81–122.
Halfen, J.A., Mahaptra, S., Wilkinson, E.C., Kardeli, S., Que Jr., V.G., Young Jr., L., Zuberbuhler, A.D., Tolman, W.B., 1996. Science 271, 1397.
Hamming, M., Foster, N., 1972. Interpretation of Mass Spectra of Organic Compounds. Academic Press, New York, USA.
Kumar, K.H., Perumal, P.T., 2007. Tetrahedron 63 (38), 9531–9535.
Lazzaroni, M., Bianchi Porro, G., 2004. Aliment Pharmacol. 20 (Suppl. 2), 48–58.
Li, T.R., Yang, Z.Y., Wang, B.D., Qin, D.D., 2008. Eur. J. Med. Chem. 43, 1688–1695.
Liu, Y.L., Ho, D.K., Cassady, J.M., Cook, V.M., Barid, W.M., 1992. J. Nat. Prod. 55 (3), 357–363.
Mehrotra, R.C., Bohra, R., 1983. Metal Carboxylates. Academic Press, London, UK.
Nakamoto, K., 1988. Spectroscopy and Structure of Metal Chelate Compounds. Springer, Berlin, p. 214.
Rice-Evans, C., 2001. Flavonoids antioxidants. Curr. Med. Chem. 8 (7), 797–807.
Sarkar, Sandipan, Dhara, Pulak K., Nethaji, M., 2009. Pabitra Chattopadhyay. J. Coord. Chem. 62, 817–824.
Shin, J.S., Kim, K.S., Kim, M.B., Jeong, J.H., Kim, B.K., 1999. Bioorg. Med. Chem. Lett. 9 (6), 869–874.
Sohel, Mostahar, Sayed, Alam, Azizul, Islam, 2006. Indian J. Chem. 45B, 1478–1486.
Sorenson, J.R.J., 1976. J. Med. Chem. 19 (1), 135–148.
Sorenson, J.R.J., 1989. Progress in Medicinal Chemistry 26, 437–568.
Swearingen, J.K., West, D.X., 2001. Trans. Met. Chem. 26, 252.